# YOUNGER DRYAS EXPERIMENTS

Daniel G. Wright & Thomas F. Stocker[1]
Department of Fisheries and Oceans
Bedford Institute of Oceanography
Dartmouth, N.S. B2Y 4A2
Canada

## Abstract

Probably the best documented climate event in which ice played a major role is the Younger Dryas. This event interrupted warming over the North Atlantic and surrounding regions during the last termination for a period of about 1000y. Broecker and colleagues suggest that the event was due to a temporary weakening or cessation of the overturning circulation in the Atlantic Basin, which presently carries more than a Petawatt of heat into this region. The change in ocean circulation may have been initiated by the input of meltwater to the North Atlantic, but the event has not been successfully modelled.

An important contribution to our knowledge of the Younger Dryas event is provided by a reconstruction of the glacial melting rates by Fairbanks (1989) who demonstrates that the Younger Dryas event occurred during a minimum in meltwater discharge. He notes the possible contradiction with the idea that melt-water caused a shut-down of the Atlantic overturning circulation.

Here, we examine the influence of meltwater discharge on a steady state solution of a simple, coupled, global ocean-atmosphere-sea ice model. If an initial state for the model experiments is obtained by spinning up to present-day conditions, then the response to meltwater input is consistent with past studies: the Atlantic overturning circulation collapses and never recovers. However, if the hydrological cycle of the initial state is modified such that there is a modest increase in net fresh water loss from the Atlantic basin, then the response to meltwater input is more consistent with reconstructions of the Younger Dryas event. Results indicate that the initial pulse of meltwater resulted in a fresh water cap over the high latitude North Atlantic which caused a shut-down of the overturning circulation in this basin. During the 'collapsed' state, air temperatures decrease and sea ice extends southward over the northern North Atlantic, qualitatively consistent with observations. With appropriate model parameters, after the meltwater pulse terminates, the fresh water cap is slowly eroded away, convection is eventually re-initiated, the sea ice melts, and the overturning circulation rapidly resumes. The second meltwater pulse described by Fairbanks has relatively little influence on the overturning circulation or the climatic conditions.

Sensitivity of results to model parameters and idealizations are examined, and limitations of the model and the solution are identified.

---

[1] Lamont-Doherty Geological Observatory of Columbia University, Palisades, N.Y. 10964, U.S.A.

NATO ASI Series, Vol. I 12
Ice in the Climate System
Edited by W. Richard Peltier

### 1. Introduction

The Younger Dryas was a brief climate event which interrupted the warm conditions accompanying the last termination, particularly around the North Atlantic and surrounding areas (Ruddiman and Duplessey, 1985; Broecker et al., 1985, 1988). This event was apparently associated with major changes in the circulation of the North Atlantic. For example, Ruddiman and McIntyre (1981) showed evidence that during the last termination, the polar front moved from its glacial position to near its present position where it remained for about 1000y, then it receded to near its glacial position for several hundred years during the Younger Dryas event, and finally returned to its present position where it has remained to the present. Also, Boyle and Keigwin (1982, 1987) show evidence based on Cd/Ca ratios in benthic foraminifers that the overturning circulation in the North Atlantic was reduced during the Younger Dryas event. Further, numerical modelling studies suggest that the observed cooling around the North Atlantic (CLIMAP, 1981) could have resulted from changes in the circulation and surface temperatures of the Atlantic basin (Broecker et al. 1985, Rind et al. 1986). Combined with recent data on the timing and rates of circulation change in the North Atlantic (Lehman and Keigwin, 1992), there seems to be little doubt that these changes played an important role in the Younger Dryas Climate event.

Broecker et al. (1988) proposed that a diversion of meltwater from the Mississippi to the St. Lawrence estuary caused a sufficient reduction in the surface salinity over the North Atlantic to stop convective overturning and the associated deep Atlantic overturning circulation. To test this hypothesis, Maier-Reimer and Mikolajewicz (1989) performed deglaciation experiments with an Ocean General Circulation Model (OGCM) which showed that only very small additions of fresh water to the Atlantic basin were required to cause a dramatic reduction in the overturning circulation and the associated northward heat flux. Even for input at the latitude of the Mississippi outlet, fresh water input at a rate of about $0.03 \cdot 10^6 m^3 s^{-1}$ was sufficient to initiate this transition. This amount is less than 10% of the maximum inflow rates during the deglaciation estimated by Fairbanks (1989). While these integrations were not carried out to steady state, the extreme sensitivity and the demonstration of multiple equilibria in OGCMs (Bryan 1986; Manabe and Stouffer 1988; Marotzke and Willebrand 1991) suggests the possibility that even if the experiments were continued after termination of the fresh water input, the system may not return to its original state. It was later shown by Stocker and Wright (1991b) that this was the case for an idealized ocean model consisting of Atlantic and Pacific basins, each represented by zonally averaged equations of motion. However, they then showed that realistic changes in the atmospheric flux of fresh water from the Atlantic to the Pacific basin could cause a re-initiation of the present-day conveyor belt circulation. Thus, it appears that a very small input of meltwater could shut down the overturning circulation in the Atlantic, and it could be re-initiated by a plausible change in the global hydrological cycle.

Before continuing it is perhaps worth discussing the cause of the extreme sensitivity of ocean models to meltwater input. As discussed by Bryan (1986), it is associated with a positive feedback between the freshening of the ocean's surface layer and the strength of the ocean's meridional overturning circulation. The essential point is that high latitude freshening will reduce the surface density in this region, and if sufficient, this can interrupt deep convection and hence increase the residence time of surface waters. For a region of net precipitation, the increased residence time results in further freshening. In fact, even if the initial input of fresh water is insufficient to eliminate convective overturning, reduced meridional overturning may still increase the residence time of surface waters and the resulting positive feedback can again lead to enhanced freshening, elimination of deep convection and major changes in ocean circulation. The relevance to the real world is emphasized by Duplessey et al. (1992) who show that such a feedback is required to account for the observational estimates of freshening during the Younger Dryas event. They note the possibility of an additional feedback involving the atmospheric branch of the hydrological cycle but, in the interest of simplicity, this possibility will not be considered here.

More recent information on the timing of Younger Dryas has further clarified the nature of the event. Fairbanks (1989) notes that Younger Dryas occurs between two maxima in meltwater input and points out the apparent contradiction with explanations that call upon maximum influxes of glacial ice and water during the event. Furthermore, the results of Fairbanks (1989) and Lehman and Keigwin (1992) make it clear that the Atlantic heat flux decreased only after the first peak in meltwater discharge which reached a maximum of order $0.5 \cdot 10^6 m^3 s^{-1}$, spontaneously re-initiated about 1000 years later when discharge rates were still of order $0.08 \cdot 10^6 m^3 s^{-1}$, and were not substantially affected by the second meltwater pulse which reached a maximum of about $0.3 \cdot 10^6 m^3 s^{-1}$. Previous attempts to model Younger Dryas would have the circulation collapse much earlier than observed and would likely recover only if the hydrological cycle were modified. This model failure has contributed to uncertainty about the role of meltwater in this event (Fairbanks 1989, 1990; Jansen and Veum 1990; Veum et al. 1992; Zahn 1992).

It is clear from the above discussion that the Atlantic overturning circulation was far more robust at the time of Younger Dryas than numerical modelling studies have suggested. Here, we examine the influence of the meltwater discharge estimated by Fairbanks on a steady state solution of an idealized model of the coupled ocean-atmosphere-sea ice system to see if the inconsistencies with previous modelling studies can be reasonably resolved. We begin in the next section with a brief discussion of the idealized model that will be used. Then, in section 3 we re-examine a typical solution of this model and its response to meltwater input, confirming the discrepancies noted above. In section 4, we introduce an alternative spin-up procedure for the model which allows us greater flexibility in the initiation of our experiments, and in section 5 we use this approach to examine the sensitivity of model results to changes in the atmospheric branch of the hydrological cycle. In section 6 we give a discussion of some of the most important model idealizations and uncertainties, and summarize results.

## 2. Model Description

The model used here is essentially the coupled ocean-atmosphere model described in Stocker et al. (1992; henceforth SWM92), extended to include a thermodynamic sea ice formulation. Each component has been described in detail in previous publications (WS91, WS92, SWM92, Semtner 1976), and hence only summary discussions of the three components will be given here.

### 2.1 The Zonally Averaged Ocean Model

The ocean model formulation is based on the zonally averaged equations developed in WS91 and the extensions and simplifications presented in WS92.

Zonally averaging the equations of motion for a single basin introduces two terms that must be parameterized. The first is the east-west pressure difference, the vertical structure of which is related to the east-west density difference through the hydrostatic relation. The latter has been parameterized using the scheme introduced in WS91/92:

$$\Delta\rho = -\varepsilon_0 \frac{\pi}{3} \sin 2\phi \frac{\partial \rho}{\partial \phi} \tag{1}$$

With this parameterization, the vertical structure of the east-west pressure difference is known, and the pressure difference at the surface is determined by the condition that the depth integral of the total north-south velocity, v (geostrophic + Ekman components) must vanish. Finally, the vertical velocity is determined from the zonally averaged continuity equation.

Second, zonal averaging yields unknown horizontal eddy fluxes of heat and salt associated with east-west variations in v, T and S. These eddy fluxes include contributions from both mesoscale eddies and the large-scale wind-driven horizontal gyre circulation. These effects are represented by horizontal eddy diffusion, but this approach is clearly limited, particularly for the large-scale gyre effects. Nevertheless, WS92 show that the two parameterizations give a reasonable approximation to the zonally-averaged ocean temperature and salinity fields, and to the meridional fluxes of heat and salt.

The Pacific, Atlantic and Indian Oceans are each represented by zonally averaged equations of motion and coupled through the circumpolar Southern Ocean as illustrated in Fig. 1. Exchange between the Southern Ocean and the other basins occurs across 40°S. Zonal exchange within the Southern Ocean is sufficiently rapid that for the time scales of interest here, the water mass properties south of each of the other basins are reasonably approximated by the zonally averaged water mass properties around the entire Southern Ocean. Thus the zonally averaged formulation remains useful in this basin and exchange with the other basins is determined exactly the same as the exchange between two cells within a single basin.

South of 55°S in the Southern Ocean, there are no continental barriers to support east-west density or pressure differences. However, such differences are supported at depth by the presence of subsurface ridges. This is particularly important when windstress is included since if no ridges were present, any north-south Ekman flux in the surface layer between cells 1 and 2 (Fig. 1) would have to be returned through bottom and internal Ekman layers, and this would require unrealistically large east-west flow in this latitude band. In the present formulation, any surface Ekman flux between cells 1 and 2 is returned geostrophically beneath the top of a subsurface ridge. In addition, purely thermohaline driven flow also develops at these depths to help transport Antarctic Bottom Water away from the continent. The modification to allow for such ridges is discussed in WS92. As done there, we use $\varepsilon_0$=0.15 beneath a ridge crest at 2500m depth. This value of $\varepsilon_0$ corresponds to a zonal separation of 180° between ridges.

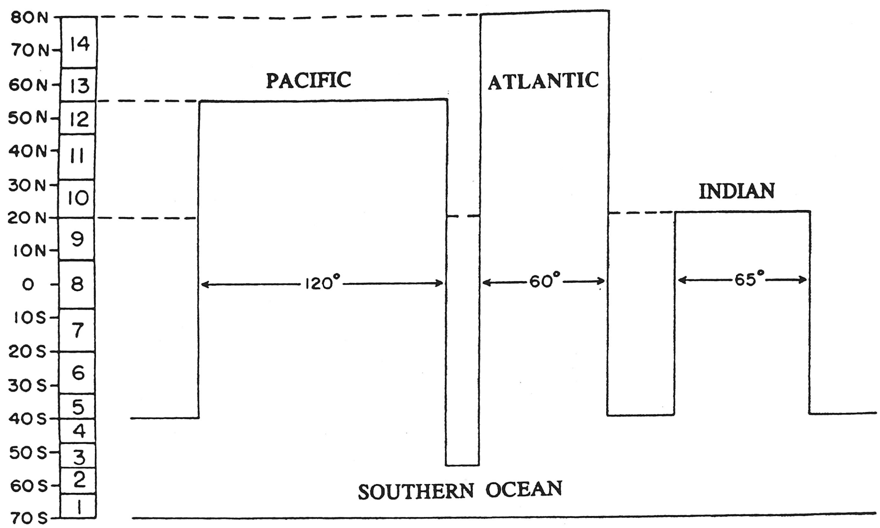


Figure 1: The idealized model representation of the global ocean. The Pacific, Atlantic and Indian Oceans are represented by 8, 10 and 5 latitude bands as indicated. Exchange between these basins occurs via the Southern Ocean which occupies the southernmost 4 bands.

The zonal mean wind stress estimates of Han and Lee (1983) are applied to the surface layer of the ocean and there is no flow and no flux of T or S through solid boundaries. During the initial spin-up, the surface layer values are restored to observations through the conditions

$$-K_V\frac{\partial T}{\partial z} = \frac{H_{mix}}{\tau}(T-T_*) \quad , \quad -K_V\frac{\partial S}{\partial z} = \frac{H_{mix}}{\tau}(S-S_*) \tag{2}$$

where $\tau = 50$d, $H_{mix}$ is the thickness of the top layer of the model which is assumed to be well-mixed, $K_v$ is the vertical diffusion coefficient, and $T_*$, $S_*$ are the zonally averaged observational estimates of T and S for the individual basins at 30m given by Levitus (1982).

The solution procedure is now relatively straightforward. The evolution of T and S are governed by the advection diffusion equations, the zonally averaged density is determined by a fully nonlinear equation of state and any static instabilities are removed through a convective overturning scheme that guarantees stability at the end of each time step (WS92). The new velocity field is diagnosed from the density field as described above and the procedure is repeated to march through time.

After a steady state is obtained, it is desirable to account for the different nature of heat and fresh water fluxes across the surface in transient experiments. In one popular approach, referred to as mixed boundary conditions, the surface water flux is diagnosed from the steady state and treated as a fixed quantity during subsequent experiments while the surface temperatures are continuously restored to observed values as before. This approach has given useful insights into the different roles played by heat and water fluxes, but it suffers from some obvious limitations. Notable among these are the fact that possible evolution to a state with a different surface temperature field is limited, and the feedback of surface temperature changes on the surface water flux is also excluded. An approach which at least reduces these problems is to couple the ocean model to a simple model of the atmosphere.

### 2.2 The Energy Balance Model of the Atmosphere

The atmosphere formulation used here is discussed in detail in SWM92. An important feature of the model is that we have deliberately suppressed some atmospheric feedbacks. The model is based on the energy balance models of Budyko (1969) and Sellers (1969). All quantities are parameterized in terms of the zonally averaged (over $2\pi$) surface air temperature whose temporal evolution is governed by a forced diffusion equation: all meridional heat transport is modelled by Fickian diffusion. Forcing is by the difference in energy flux across the upper and lower boundaries.

Short wave radiation enters through the upper surface as dictated by the solar constant. Some of this radiation is scattered or reflected (off clouds, dust, ice, water, ...) back to space without ever getting involved in the earth's heat engine. In our model, we set this fraction of passing wave energy at its present-day, latitude-dependent value (Stephens et al., 1981) and consider only the fraction of energy (about 70%) that interacts with the climate system. Outgoing long wave radiation is parameterized as simple grey body radiation in terms of the surface air temperature with the latitude dependent emissivity chosen to be consistent with observational estimates of the outgoing longwave radiation (Stephens et al., 1981).

Of the short wave energy that actually interacts with the climate system, 2/7ths is taken to be absorbed directly into the atmosphere while the remainder is absorbed into the surface layer of the ocean or land. Heat storage in the land surface is neglected so the net incoming shortwave over the land is effectively absorbed into the atmosphere although in reality it enters as long wave energy after heating the land surface. It is important to note here that the fraction of short wave energy that is reflected off the earth's surface has already been accounted for at the top of the atmosphere, and we are deliberately neglecting albedo feedbacks associated with changing clouds, humidity, ice, etc. Heat and moisture exchanges are affected by the presence of sea ice as discussed in the next subsection.

Air-sea heat exchange occurs via the downwelling short wave radiation discussed above, upwelling and downwelling of long wave radiation, sensible heat flux and latent heat flux. Each of these is parameterized in terms of the ocean and atmosphere surface temperatures and the model is fit to present day observations by using results diagnosed from our ocean model, spun up under restoring boundary conditions, plus observational estimates of the annually and zonally averaged surface air temperatures (Oort, 1983) and of evaporation from each of the ocean basins (Baumgartner and Reichel, 1975). Upwelling radiation from the ocean surface is represented as grey body radiation with a constant emissivity of 0.96, the sensible heat flux is linearly related to the air-sea temperature difference with a proportionality constant of $10\mathrm{W}/(\mathrm{m}^2\mathrm{K})$ and the latent heat flux is parameterized as a function of the surface air temperature and the air-sea temperature difference. The functional dependence of the latter exchange is taken from Haney (1971) while a latitude dependent proportionality constant is chosen to agree with present day estimates of evaporation over each of the ocean basins (Baumgartner and Reichel, 1975). By fixing these bulk coefficients we neglect feedbacks associated with changing wind speeds and atmospheric stability. Finally, downwelling long wave radiation is parameterized as grey body radiation in terms of the surface air temperature with the latitude dependent emissivity chosen to be consistent with the previously determined components plus the net air-sea heat flux diagnosed from the ocean model under restoring boundary conditions. Again, feedbacks associated with changing moisture content, etc are neglected.

Moisture storage in the atmosphere would be small in reality and is neglected in our model. Thus, changes in evaporation during transient runs must be compensated by changes in precipitation. Here we use the simplest possible closure scheme and assume that changes in evaporation are locally compensated by changes in precipitation. Note that this approach allows for the effect of varying air-sea latent heat exchanges but eliminates possible feedbacks associated with net changes in interbasin water fluxes.

Finally, the horizontal diffusion coefficients for the atmosphere are chosen to be consistent with the present-day meridional distribution of heat in the atmosphere and the heat sources and sinks discussed above.

### 2.3 The Thermodynamic Sea Ice Model

At the time of coupling, sea ice is not present in our ocean model but it is subsequently allowed to develop. The Arctic basin is not explicitly included, so we are effectively assuming that sea-ice conditions over this basin remain constant. The neglect of all other ice in our present-day simulation is clearly an over-simplification that reflects the level at which we are attempting to model sea ice changes. With our zonally averaged model, we cannot account for east-west variations in ice extent and hence any formulation we use will necessarily be fairly crude. However, for climate simulations, we must still include a formulation which will (i) limit temperatures to be at or above the local freezing point, (ii) provide insulation against further heat loss as the ice thickens, and (iii) eject salt into the surface layer during freezing and add fresh water to this layer on melting. To incorporate these basic characteristics in the simplest manner possible, we use the 'zero layer' thermodynamic sea ice model developed by Semtner (1976). Partial ice cover of a grid cell is allowed for, but we do not consider modifications due to snow cover, penetration of solar radiation or melting of internal brine pockets. The annually averaged forcing used here does not allow for potentially important seasonal variations in sea-ice although this effect could be incorporated, and work on this aspect is in progress.

Given the surface fluxes through the ice-covered and ice-free portions of a cell (see below) we proceed as follows. In the ice covered regions, if the temperature drops below the local freezing point, we simply create sufficient ice on the bottom of the existing ice to bring the temperature to the freezing point. Similarly, if the water temperature exceeds the local melting point, we melt ice from the bottom until either no ice is left or the temperature is reduced to the melting point. In open areas, ice forms when the surface water temperature drops below the freezing point. Initially, ice forms at a thickness of 0.4m over an area sufficient to bring the temperature back to the freezing point. If the resulting fraction of ice cover for the grid cell exceeds the maximum allowable (0.995), then the excess ice is added to the bottom of the existing ice. If the surface temperature of the open water region exceeds the melting point, ice is melted from the side of any existing ice until either no ice remains or the temperature is reduced to the melting point. In all cases, ice is taken to have zero salinity and salt is conserved through exchange with the surface layer of the ocean. After both ice-covered and ice-free regions have been adjusted as above, the ice thickness is reset to the average value over the new ice-covered region, and the temperature and salinity of the surface layer are set to the average values over the entire cell.

Surface heat fluxes are updated at the end of each time step. For ice-free portions of a cell the heat flux is determined exactly as for a cell in which there is no ice. The flux through the ice-covered portion of a cell is determined through a two step procedure. First, the surface temperature of the ice is updated to the equilibrium value, $T_i^n$, at which the diffusive flux through the ice balances the radiative and sensible fluxes from the surface of the ice to the atmosphere (the latent heat flux across the surface of the ice is neglected). Linearizing the resulting equation about $T_i^{n-1}$, the surface temperature of the ice at the end of the previous time step, this gives

$$T_i^n = T_i^{n-1} - \frac{\sigma e_O (T_i^{n-1})^4 - \sigma e_A (T_A^n)^4 + D_{ia}(T_i^{n-1} - T_A^n) - \frac{\mathrm{K}_i}{h_i}(T_f - T_i^{n-1})}{4\sigma e_O (T_i^{n-1})^3 + D_{ia} + \frac{\mathrm{K}_i}{h_i}} \tag{3}$$

where $T_f$ is the local salinity dependent freezing temperature (Gill 1982, p.602), $h_i$ and $K_i$ are the ice thickness and diffusivity, $D_{ia}=10\mathrm{Wm}^{-2}$ is an exchange coefficient which linearly relates the sensible heat flux across the surface of the ice to the difference between the surface ice temperature and the surface air temperature, and all temperatures are in degrees Kelvin. If $T_i^n$ is below the freezing point, this determines the new surface temperature of the ice and the corresponding ice to atmosphere heat flux equals the diffusive heat flux through the ice:

$$F_i^n = \frac{\mathrm{K}_i}{h_i}(T_f - T_i^n). \tag{4}$$

If $T_i^n$ is above the melting point, then ice must melt until a new equilibrium is achieved. At this new equilibrium, the surface temperature of the ice will be at the melting point, $T_m$. The heat flux is thus given by

$$F_i^n = -(1-\kappa)S + \sigma e_O T_m^4 - \sigma e_A T_A^4 + D_{ia}(T_m - T_A), \tag{5}$$

and the corresponding ice thickness by

$$h_i = \frac{\mathrm{K}_i (T_f - T_m)}{F_i^n}. \tag{6}$$

Any melting results in fresh water at the melting temperature which is added to the surface layer.

This completes a time step for the sea ice. Since sea ice can respond to atmospheric changes on a time scale of a few days, whereas the time step for the ocean is typically 10 days, sea ice is updated on the same time step as the atmosphere (about 0.5 days). Due to the effect on sea ice of conditions in the surface layer of the ocean, we must also update the surface layer on this time step. To do this without greatly increasing the computational burden, we have taken the fluxes across the bottom and side walls of each surface cell to be constant over an oceanic time step and only allowed the surface flux to vary over the shorter atmospheric time step.

## 3. 'Typical' response to meltwater input

Model results for the Atlantic basin corresponding to the standard parameter values listed in Table 1 are presented in Fig. 2. These results, as well as those for the other basins, are very similar to those presented in WS92. They correspond to the steady state obtained after 5000y of spin-up under the restoring boundary conditions (2). The values of $T_*$ and $S_*$ used were the zonally averaged values at 30m compiled by Levitus (1982) except in the southernmost latitude band where $S_*$ is increased to 34.6 and in the northernmost cell of the North Atlantic where $S_*$ is increased to 35. These values correspond roughly with those of the deep water massses formed during winter.

The large scale overturning circulation is qualitatively consistent with the global conveyor belt circulation described by Gordon (1986). Deep water is formed primarily in the northern North Atlantic

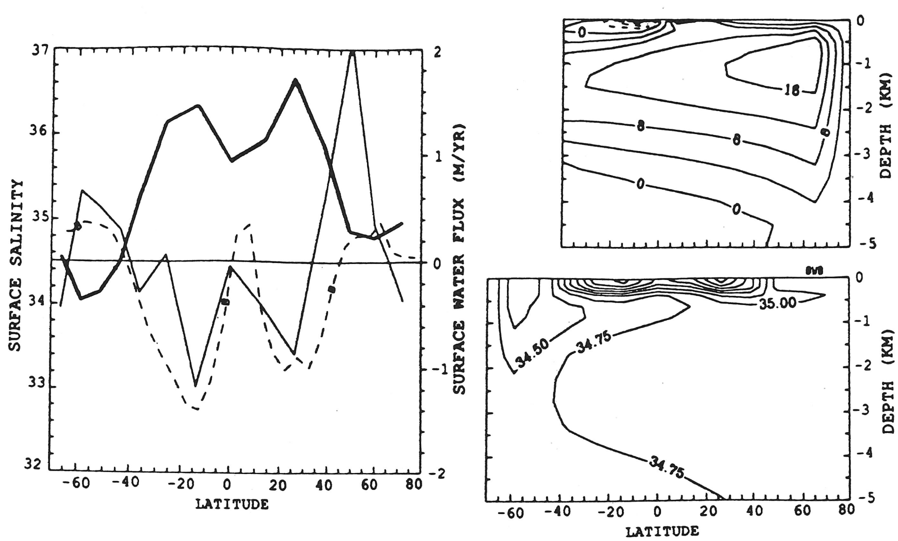


Figure 2: Model results for the case in which surface values of T and S are restored to present-day conditions. (a) The surface salinity (heavy line), the surface water flux (light solid line) and Baumgartner and Reichel's estimates of the local surface water flux, excluding runoff (broken line). (b) The stream function in $10^6 m^3 s^{-1}$. (c) The salinity in parts per thousand.

Table I: Model Parameters

| Ocean Parameters | | |
|---|---|---|
| $a$ | Earth's radius | 6371 km |
| $g$ | Earth's gravitational acceleration | 9.81 $m/s^2$ |
| $f$ | Coriolis parameter | $2\Omega\sin\phi$ |
| $\Omega$ | Earth's angular velocity | $7.27\cdot10^{-5}$ $s^{-1}$ |
| $H$ | ocean depth | 5000 m |
| $\rho_*$ | reference density | 1027.8 $kg/m^3$ |
| $D_{oa}$ | sensible heat exchange coefficient | 10 $W/(m^2K)$ |
| $K_H$ | horizontal eddy diffusivity | 500 $m^2/s$ |
| $K_V$ | vertical eddy diffusivity | $0.44\cdot10^{-4}$ $m^2/s$ |
| $\varepsilon_0$ | closure parameter for 60° basin | 0.45 |
| $\tau$ | restoring time for surface layer | 50 days |
| $C_o$ | specific heat capacity of sea water | 3900 J/(kgK) |
| $e_o$ | ocean surface longwave emissivity | 0.96 |
| $H_{mix}$ | surface layer depth | 50 m |
| cell interface depths [m] | | 50, 100, 150, 250, 500, 750, 1000, 1250, 1500, 2000, 2500, 3000, 3500, 4000, 4500, 5000 |

| Atmospheric Parameters | | |
|---|---|---|
| $\rho_A$ | surface air density | 1.225 $kg/m^3$ |
| $C_A$ | specific heat capacity of dry air | 1004 J/(kgK) |
| $H_A$ | scale height | 8320 m |
| $\sigma$ | Stefan-Boltzman constant | $5.67\cdot10^{-8}$ $W/(m^2K^4)$ |
| $\kappa$ | absorptivity of shortwave radiation | 2/7 |
| $D_{wa}$ | transfer coefficient for sensible heat | 10 $W/(m^2K)$ |
| $L$ | latent heat of evaporation | $2.5\cdot10^6$ J/kg |
| $e_P$ | planetary emissivity | † footnote |
| $e_A$ | atmospheric emissivity (downwelling) | † footnote |
| $c_E$ | bulk coefficient for evaporation | † footnote |
| $K_A$ | horizontal eddy diffusivity | † footnote |

† These parameters are chosen to fit the atmospheric component of the model to present-day observations as discussed in Stocker et al. (1992).

| Ice Parameters | | |
|---|---|---|
| $\rho_i$ | ice density ($0.9\cdot\rho_*$) | 925 $kg/m^3$ |
| $q_i$ | latent heat of fusion | $3.34\cdot10^5$ J/kg |
| $K_i$ | ice conductivity | 2 W/(mK) |
| $T_f$ | freezing point | S-dependence from Gill (1982) |
| $T_m$ | melting point | -0.1°C |
| $e_i$ | ice surface longwave emissivity | 0.96 |
| $D_{ia}$ | sensible heat exchange coefficient | 10 $W/(m^2K)$ |

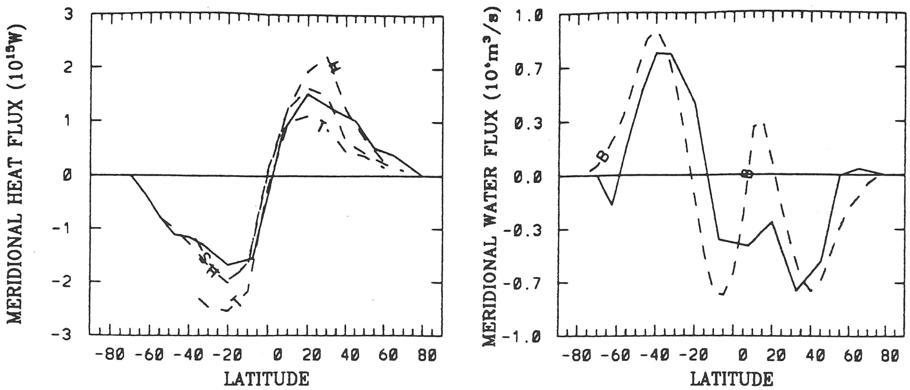


Figure 3: (a) Model estimate of the total heat carried by all oceans (solid line) compared with observational estimates by Hastenrath [1982] (H), Talley [1984] (T) and Hsiung [1985] (S). (b) Model estimate of the total atmospheric water flux compared with the estimate of Baumgartner and Reichel [1975] (B).

and around Antarctica, while broad upwelling occurs over much of the remainder of the global ocean. The corresponding zonally averaged temperatures and salinities also compare well with observations except in locations which are directly influenced by marginal seas, where there are significant differences in the salinity field. However, as discussed in WS92, explicit inclusion of the marginal seas (their effect is implicitely felt through the restoration to observed surface values) does not appear to have a global effect.

The model estimates of the global oceanic meridional heat transport and atmospheric water transport implied by the diagnosed surface fluxes are shown in Fig. 3 and are in reasonable agreement with observational estimates.

One question of obvious interest to us is how much fresh water flux into the North Atlantic is required to shut down or reverse the overturning circulation. Some idea of the robustness of the overturning circulation can be obtained by subjecting a steady state solution to a continuously increasing input of freshwater until the circulation collapses. Figure 4c shows the northward heat flux carried by the overturning circulation across 32.5°N in the Atlantic Ocean for two different model runs. The heat flux is shown here because it is a good proxy for the overturning circulation in the North Atlantic and it gives an immediate indication of the climatic significance of changes in this quantity. In the following we consider two cases of different surface boundary conditions. In the first case mixed boundary conditions are applied, while in the second case we consider the coupled model and hence include more realistic feedback mechanisms between the ocean and the atmosphere. In each case, the initial state of the ocean is steady before the fresh water flux perturbation is initiated. This perturbation is initiated at t=1000y, and is added to the Atlantic between 20° and 32.5°N. At t=1000 the fresh water flux perturbation vanishes and afterwards it increases by $0.1 \cdot 10^6 m^3 s^{-1}$ every 1000y. The slow increase in input is intended to allow us to estimate the maximum sustained freshwater input that can be tolerated.

Each of the cases considered is initiated with the state illustrated in Figs. 2 and 3. The case represented by the broken line corresponds to the run performed under mixed boundary conditions (temperature restored to observed values while the surface water flux is fixed at its initial value plus the temporally varying input described above). As the input of freshwater to the North Atlantic increases between years 1000 and 1500, the overturning circulation decreases slightly, consistent with the slight decreases in surface salinity and temperature over this interval (Fig. 4a,b,c). Between t=1500 and t=1600 years, both salinity and temperature decrease more rapidly. Evidently, the temperature decrease is insufficient to compensate for the buoyancy change associated with the decrease in salinity

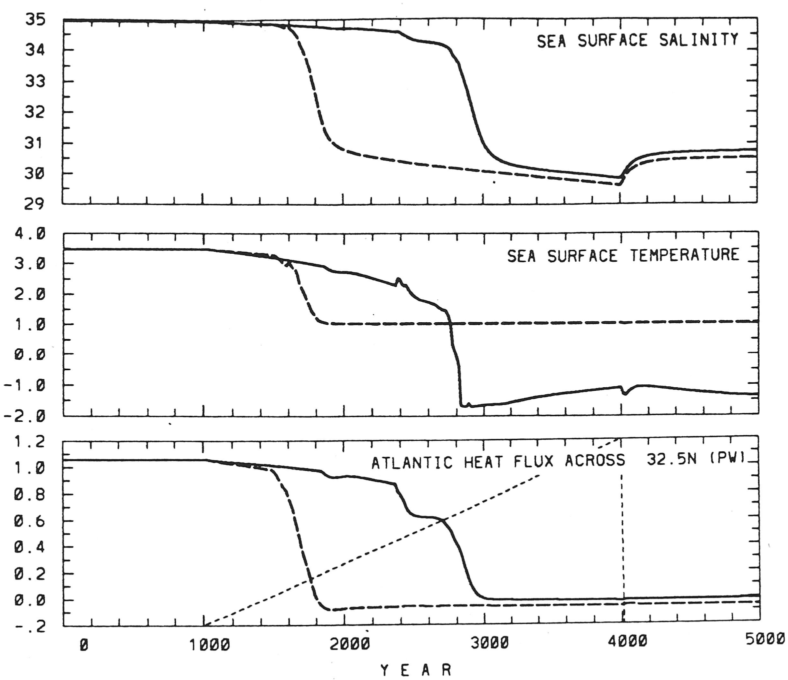


Figure 4: Model results for runs in which the fresh water is added to the North Atlantic basin between 20 and 32.5N and varies between 0 and $0.3 \cdot 10^6 m^3 s^{-1}$ as indicated by the light broken line in panel c. Heavy broken lines correspond to a run with surface temperatures restored to observed values and solid lines correspond to the coupled ocean-atmosphere-sea ice formulation. (a) Surface salinity and (b) surface temperature in the northernmost model cell of the North Atlantic. (c) The meridional heat flux carried by the Atlantic basin across 32.5N.

and convection is essentially eliminated in the northernmost cell of the North Atlantic by t=1600y. The North Atlantic heat flux across 32.5°N decreases by about 20% between years 1500 and 1600 and beyond year 1600 (input rate of $0.06 \cdot 10^6 m^3 s^{-1}$), precipitous decreases in salinity, temperature and heat flux are observed. By year 2000 the surface salinity has decreased by 4ppt, the temperature by 2.5°C and the heat flux across 32.5°N has decreased to a slightly negative value.

One obvious question about the above experiment regards the validity of applying the restoring boundary condition to surface temperature during such a transient run. For example, Zhang et al. (1992) show that replacing this condition with a zero heat capacity atmosphere acts to stabilize their model against an isolated *pulse* of fresh water (note that this does not guarantee stability with respect to sustained fluxes as considered here). Their use of a zero heat capacity atmosphere permits unrealistically rapid adjustments in the surface air temperature, but results nevertheless demonstrate the importance of allowing the surface temperature to adjust realistically during transient runs.

The second case illustrated in Fig. 4 (solid curves) is identical to the first except that the mixed boundary conditions have been replaced by the coupled ocean-atmosphere-sea ice formulation. It is immediately apparent that the change in surface boundary condition has delayed the collapse of the overturning circulation by about 1200 years. The salinity decrease of about 0.9ppt before the abrupt collapse is substantially greater than that for the previous case due to the greater ability of the surface temperature to compensate for salinity induced buoyancy changes. However, eventually convective overturning is again greatly reduced, the salinity and temperature decrease rapidly, and the heat flux

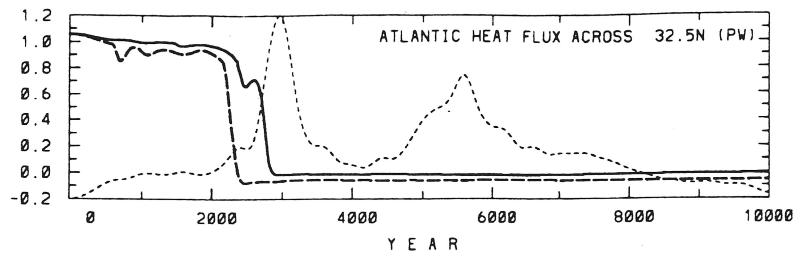


Figure 5: Analogous to figure 4(c), but in this case the freshwater input is specified in accordance with Fairbanks' estimate of meltwater input (light broken line with a range of 0 to $0.45 \cdot 10^6 m^3 s^{-1}$).

again decreases to a slightly negative value. Note that the surface temperature decrease is substantially larger for the coupled run. The 1200 year delay of the collapse corresponds to an increase in critical fresh water flux perturbation from 0.06 to about $0.18 \cdot 10^6 m^3 s^{-1}$, a substantial difference.

In each of the above experiments, the fresh water flux anomaly was set to zero beyond t=4000y to see if the initial state would be re-established. In each case, a new equilibrium was established in which the overturning circulation and the corresponding heat fluxes were similar to the states at the time when the fresh water flux was terminated, demonstrating the existence of multiple equilibria for the chosen parameter values.

Finally, Fig. 5 shows the results of an experiment in which the meltwater input estimated by Fairbanks (1989) is applied to the steady state solution considered above. Again the collapse is delayed for the coupled run. However, even for this case, it occurs at a time when the meltwater input is only of order $0.25 \cdot 10^6 m^3 s^{-1}$. This value is larger than the value of $0.18 \cdot 10^6 m^3 s^{-1}$ found in the previous experiments due to the much more rapid increase in freshwater input. The overturning circulation and the associated heat flux are essentially eliminated by year 2800 and the system never returns to its original state.

## 4. Hybrid Boundary Conditions

Clearly the experiments discussed above do not simulate the Younger Dryas climate event: most notably, the overturning circulation collapses well before the first meltwater peak and never recovers after it is shut down. Stocker and Wright (1991b) obtained a similar result in a two basin configuration and showed that a reasonable change in the atmospheric branch of the hydrological cycle could re-establish the overturning circulation. Based on their results, it is obvious that one could construct a *temporally varying* hydrological cycle such that the overturning circulation would evolve in a manner consistent with reconstructions of the Younger Dryas event.

Here we take a different approach and attempt to determine a *fixed* hydrological cycle which permits the major features of the Younger Dryas event to be reproduced by varying only the meltwater input. We will show that such a modified hydrological cycle does exist, and it is not far from the present state (the meaning of the latter qualitative statement will become clear below).

In our search for an appropriately modified hydrological cycle, it is desirable to be able to make changes in some part of the domain and determine a new equilibrium state corresponding to this modification. This requires a modification of the hydrological cycle over the remainder of the domain such that there is no net addition or removal of water from the global ocean. It is further required that the resulting state remain in the 'conveyor belt' mode of circulation consistent with reconstructions of the position of the polar front (Ruddiman and McIntyre 1981) and the meridional circulation (Lehman and Keigwin, 1992) prior to the Younger Dryas.

One way to achieve both of these goals is to introduce *hybrid boundary conditions* in which the virtual salt flux (or fresh water flux) is specified over one portion of the global ocean, but the salinity is restored to a preferred state over the remainder of the ocean surface. By restoring to values consistent with the present state, one can reduce the likelihood of a switch to an alternative equilibrium in which the global conveyor circulation is 'off', and the use of restoring boundary conditions over part of the domain allows adjustment to a new equilibrium in which a global salt (or fresh water) balance is achieved.

How and where should the hydrological cycle be modified? From the experiments discussed in the previous section, it is evident that whatever modifications we choose to make, they must increase the stability of the global conveyor belt. We have chosen to do this by decreasing the net input of fresh water to the North Atlantic. Some indication that changes in this direction are appropriate is found in Zaucker (1992) but large uncertainty remains (Kutzbach and Guetter 1986; Miller and Russell 1990). The present study examines one possible stabilizing effect: others should be considered in future studies.

To determine an initial state with appropriately reduced freshwater input to the North Atlantic we begin with an extreme case. Thus, we first consider the effect of entirely shutting off runoff into the North Atlantic. The solid line in Fig. 2 shows the model estimate of the net fresh water input over the Atlantic basin while the broken line shows the corresponding estimates of evaporation minus precipitation taken from Baumgartner and Reichel (1975). At least three effects contribute to the differences between these two sets of curves. First, our model is highly idealized and there are certainly errors in the diagnosed surface fluxes. Second, the observational estimates are subject to large uncertainties, particularly in the southern hemisphere where estimates of precipitation are unreliable. And third, the model estimates implicitly include the effect of runoff while this has not been included in the observational estimates. Note that runoff does not influence the deep ocean circulation until it

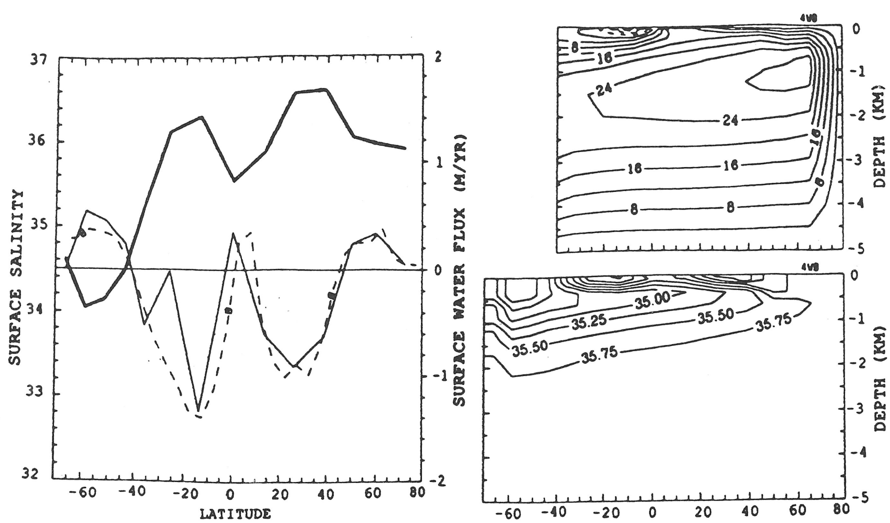


Figure 6: Model results analogous to Fig. 2 ($R$=1) but for no North Atlantic 'runoff' ($R$=0). (a) Surface salinity (heavy line) and surface water flux (light solid line). Baumgartner and Reichel's estimates of the local surface water flux (excluding runoff) are shown as a broken line. (b) The stream function in $10^6 m^3 s^{-1}$. (c) The salinity in parts per thousand.

gets off the shelf into the deep ocean and hence an appropriate distribution of runoff for a model that does not include continental shelves is difficult to estimate. For notational convenience, we shall refer to the difference between the two curves in Fig. 2 as *runoff*, but it is important to remember that model and data errors also contribute to this difference.

The new initial state obtained under the hybrid boundary conditions in which *runoff* is entirely shut off over the North Atlantic and salinity is restored to present day values is illustrated in Fig. 6. In this and all other initial states considered here, the restoring temperatures remain those of the present state. Reduced fresh water input to the North Atlantic has resulted in substantially more saline North Atlantic Deep Water and a stronger overturning circulation. In adjusting to a new equilibrium, the mean salinity of the global ocean has also increased by nearly 1ppt, fortuitously in reasonable agreement with the salinity increase expected due to the development of continental ice sheets.

Of course, there is no reason to believe that completely eliminating North Atlantic runoff yields an appropriate initial state for Younger Dryas experiments, so additional experiments in which the runoff into the North Atlantic is taken to be some fraction of the present amount will also be considered. Initial states spanning the range bounded by those shown in Figs. 2 and 6 are obtained by integrating the model under hybrid boundary conditions, with the North Atlantic surface water flux, $F$, given by

$$F = R \cdot F^{diag} + (1-R) \cdot F^{obs} \quad , \tag{7}$$

where $F^{diag}$ is the flux diagnosed from the steady state obtained by restoring to observed surface salinities (Fig. 2), $F^{obs}$ is the observed water flux (Fig. 6), and $R$ is a weight parameter with a value between 0 and 1.

After a new equilibrium has been determined, the ocean component of the model is coupled to the energy balance model of the atmosphere, and the response to transient meltwater input is examined. Results are discussed in the next section.

## 5. Response to Transient Meltwater Input

Figure 7 illustrates model estimates of the North Atlantic heat transport during meltwater input for several values of $R$. For $R$=1, the results of past studies are qualitatively reproduced in that meltwater input causes the Atlantic overturning circulation to collapse and a new steady state is approached. The time of the abrupt collapse is delayed due to the coupling to an energy balance model of the atmosphere, but the qualitative nature of the evolution is unchanged. For $R$=0.55 or smaller the overturning circulation weakens, but a complete collapse never occurs, and the initial state is re-established as the meltwater input diminishes. For $R$=0.75, a collapse occurs, but the overturning circulation returns abruptly after about 7000 years. For values of $R$ between 0.75 and 0.55 the model estimate of the duration of Younger Dryas decreases with decreasing $R$.

Choosing $R$=0.65 gives a representation of the Younger Dryas climate event and its relation to the meltwater input which is qualitatively consistent with paleoclimate records. From Fig. 8 we see that after the meltwater input begins, the salinity in the northern part of the North Atlantic decreases slowly until convection starts to decrease. As convection decreases, the surface salinity decreases more rapidly and the overturning circulation begins to collapse. This contributes further to the surface freshening by increasing the residence time of high latitude surface waters in an area of net precipitation, and the deep overturning circulation is completely eliminated in a few centuries. The reductions in convection and overturning each reduce the heat flux into the surface layer, which cools to the freezing point. The relatively low surface salinities prevent convection from being re-initiated and further cooling is limited by the growth and insulating effect of sea ice.

During the Younger Dryas event, the temperature stratification at high latitudes is unstable (the surface and deep potential temperatures are at the freezing point and near 3°C, respectively) but the density field is stabilized by the salinity stratification. After the first meltwater pulse is over, the surface salinity at middle and low latitudes in the North Atlantic increases as a result of net evaporation

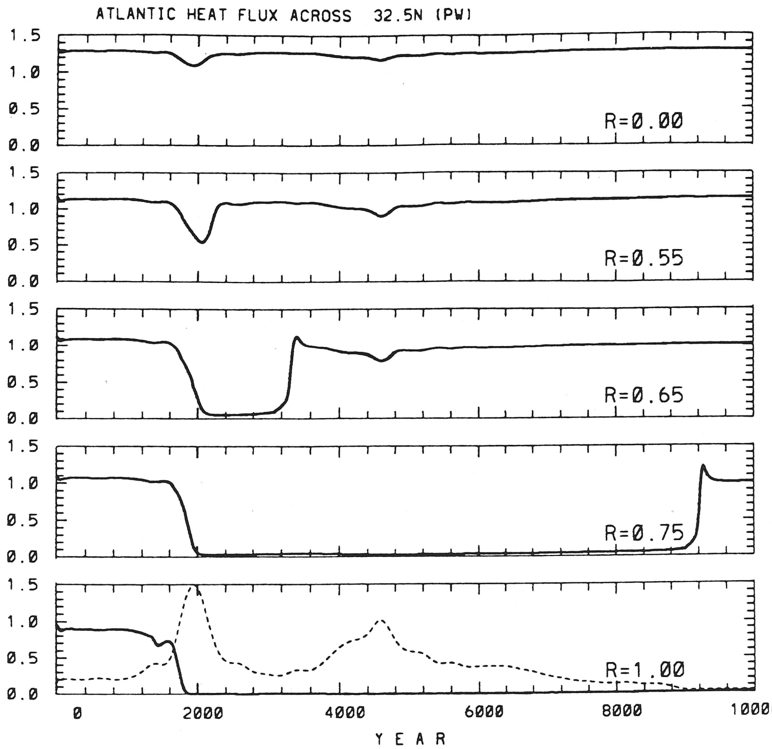


Figure 7: The heat flux across 32.5°N in the Atlantic basin for $R$=1.0, 0.75, 0.65, 0.55 and 0.0. In each case the ocean model is integrated to steady state under the hybrid boundary conditions. Then, at t=0, it is coupled to the atmospheric model component and Fairbanks' meltwater input is initiated. The meltwater is added between 20 and 32.5°N at the rate indicated by the light broken line in the bottom panel (range of 0 to $0.45 \cdot 10^6 m^3 s^{-1}$).

sufficient to overwhelm the small amount of meltwater during this period. The relatively fresh surface layer at high latitudes is slowly eroded away through exchange with the lower latitudes until the salinity stratification is insufficient to counteract the unstable temperature stratification and convection is initiated. The convection brings relatively warm, saline waters up to the surface which helps eliminate the sea ice and increase the surface salinity. Since excess heat is quickly removed, the increased surface salinity leaves the surface layer even more unstable. Once the sea ice is removed, this positive feedback results in a very rapid increase in the surface salinity to near the deep water value. As the surface salinity increases, the deep overturning circulation is re-established and the northward heat flux and convection return to values similar to those of the initial state. Once the overturning circulation is re-established, the reduced residence time of high latitude surface water serves to maintain relatively high surface salinities so that convective activity and the overturning are sustained.

During the second meltwater pulse, the surface salinity decreases much less, convection is not interrupted and the climatic impact is minor. An additional experiment in which the first meltwater pulse was eliminated also showed minimal response to this pulse. Hence the reduced response to the second pulse is not due to modified conditions as a result of the first pulse. Rather, the second pulse simply does not exceed the threshold at which convection and the overturning circulation are

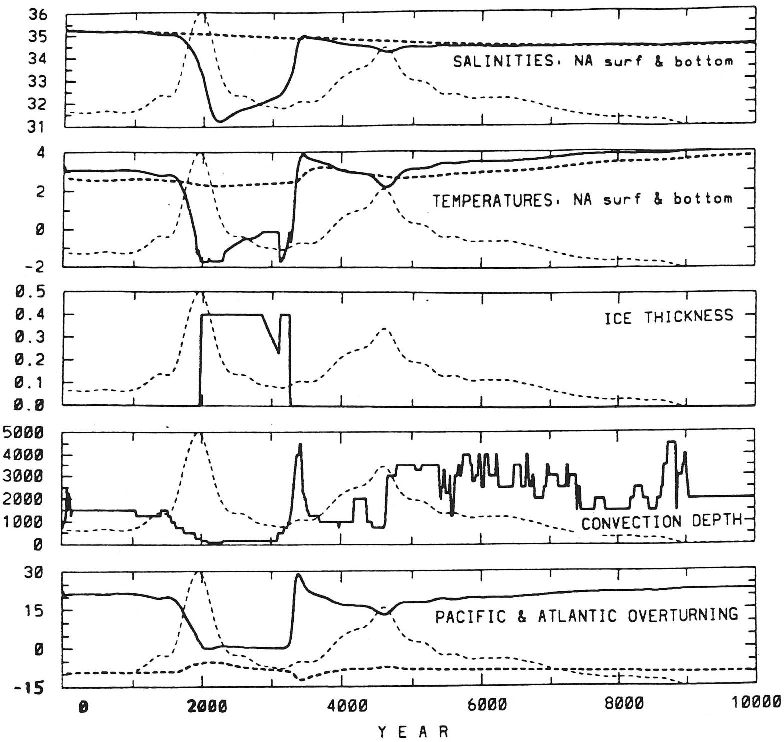


Figure 8: The evolution of model properties for $R$=0.65. The light broken curve on each panel shows the meltwater input (range of 0 to $0.45 \cdot 10^6 m^3 s^{-1}$). Panels (a)-(d) each correspond to the region north of 65N in the Atlantic basin: (a) surface (solid) and deep (>3000m; broken) salinity; (b) surface (solid) and deep (>3000m; broken) potential temperature; (c) ice thickness in meters ( the fraction of ice cover remains near 1 over most of the period when ice is present); (d) depth of convection. The maximum values of the stream functions below 1000m (away from the region dominated by wind-forced motions) north of 40°S for the Atlantic (solid) and the Pacific (broken) in $10^6 m^3 s^{-1}$ are shown in (e).

eliminated. It is of interest that if more ice had accumulated during the Younger Dryas, than the second meltwater pulse would have been stronger, and an oscillation analogous to that described by Birchfield (1990) may have occurred.

In Fig. 9 we show the overturning circulation and salinity for the Atlantic basin before, during and after the model's Younger Dryas event. The final state is similar to the initial state. Clearly the model Younger Dryas event is associated with the elimination of the thermohaline circulation in the Atlantic, and substantial weakening of the deep circulation in the Pacific (Fig. 8e). Sea surface temperature changes in the Pacific are much smaller than those in the Atlantic (<1°C cooling for our northernmost cell), but the inflow of Antarctic Bottom Water was greatly reduced in our model simulation of the Younger Dryas. There should be an observable influence of reduced nutrient supply to the surface layer if this aspect of the simulation is correct. We emphasize however that while there is evidence that Younger Dryas was a global event, (Kallel et al. 1988, Kundrass et al. 1991), caution should be exercised in interpreting this aspect of the present model. This point is discussed further in the next section.

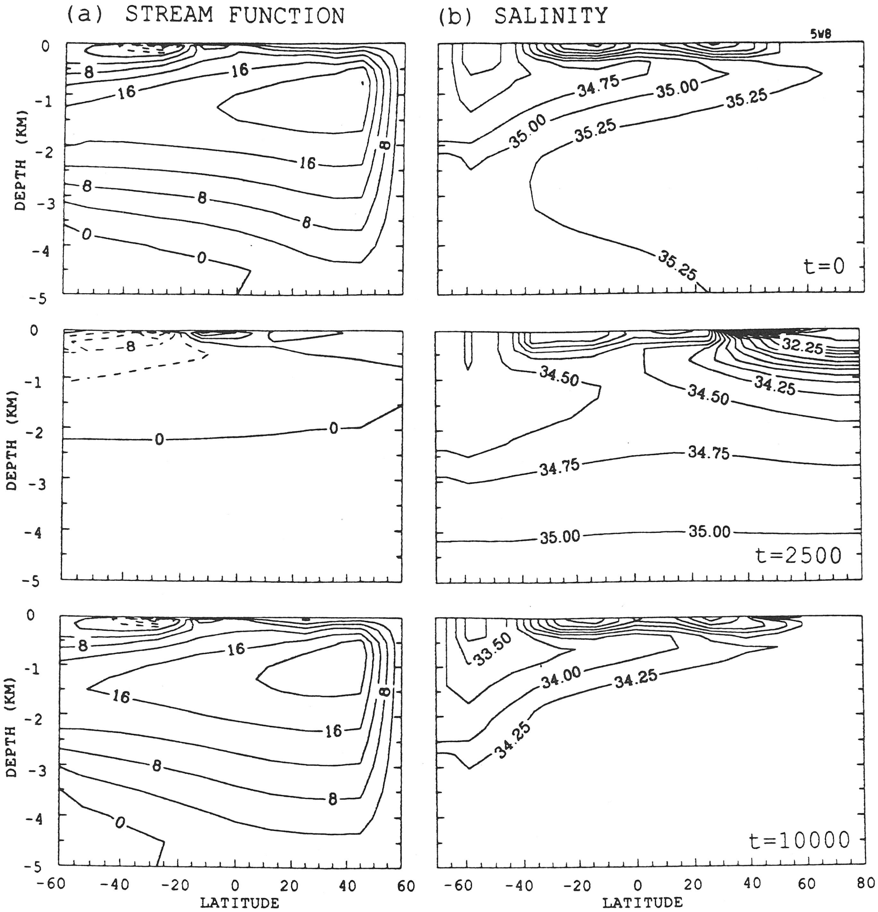


Figure 9: The Atlantic overturning circulation and salinity fields corresponding to $R$=0.65 at the initiation of meltwater input (t=0), during the model's Younger Dryas event (t=2500) and at the end of the model run (t=10,000). Note that in spite of the change in surface water flux into the North Atlantic, both the initial and the final states are qualitatively consistent with present-day conditions with the largest difference being the change in mean salinity.

## 6. Discussion and Conclusions

The use of zonally averaged equations to represent both the oceans and the atmosphere is the most obvious limitation of the present model. For the ocean, this means that some truly 3D effects such as the eddy-like feature discussed by Winton (this volume) are ommitted, and the rapid exchange via western boundary currents is represented in terms of either the zonally averaged flow or horizontal diffusion. These exchanges will thus be slowed and this should be kept in mind. This influences the detailed temporal evolution of our model predictions but our major results are unlikely to be seriously affected.

The effect of zonal averaging in the atmosphere may represent a bigger problem. In reality, when the overturning circulation in the North Atlantic is shut down, the associated temperature changes tend to be concentrated around the Atlantic basin and over Europe (Broecker et al. 1985, Rind et al. 1986). However, the use of a zonally averaged atmospheric model results in changes in surface heat flux being felt uniformly all around a latitude band. Thus, temperature changes over the North Atlantic are underestimated while those over the North Pacific are overestimated. In the Atlantic, the increased temperature will reduce the net ocean to atmosphere heat flux and may result in an early collapse of the overturning circulation. [Recall from section 3 that the small atmospheric temperature changes due to the use of an energy balance model rather than restoring temperatures were sufficient to significantly delay the collapse of the overturning circulation.] In the Pacific basin, our model estimates of atmospheric temperature during Younger Dryas will tend to be too low and this will increase the strength of the northern overturning cell in this basin. In extreme cases, these effects could result in a reversed conveyor belt circulation, but this did not occur in any of our simulations. An improved atmospheric model is clearly desirable, particularly if the global nature of Younger Dryas is of interest. A 2D EBM for the atmosphere (North et al. 1983) would be a worthwhile modification that would retain computational efficiency. Of course, there would still be uncertainties associated with the need to parameterize all atmospheric quantities in terms of the surface air temperature.

Neglected feedback mechanisms are also potentially important. In particular, we neglect changes in wind stress and the associated basin-scale gyre circulations. We also neglect changes in surface albedo, planetary emissivity, and the bulk coefficients for sensible and latent heat fluxes. All of these would certainly change through the time period considered here. The net effect of these changes depends on interactions between the various elements of the climate system. We chose to neglect feedbacks associated with these aspects of the climate system so that they play no role rather than an uncertain role.

In all of our experiments we have used Fairbanks' meltwater estimates based on $^{14}C$ dating of coral reefs and we've assumed that all meltwater enters the North Atlantic between 20 and 32.5°N. Each of these approximations deserves further investigation. As an extreme example to illustrate the potential significance of the detailed temporal structure of the meltwater input, it is apparent from section 3 that if the ice sheets were to melt sufficiently slowly, there may be no significant Younger Dryas event at all. One should not necessarily expect to find a Younger Dryas-like event at the termination of every ice age. Rapid terminations are likely slowed by such events, while slower terminations may proceed unimpeded. On the other hand, it is possible that a large rapid injection of fresh water at high latitudes could shut down convection and the overturning circulation in a situation that would otherwise withstand the meltwater input.

Finally, our initial state is a crude approximation to conditions at the beginning of Younger Dryas. We have totally neglected the presence of the large continental ice sheets and modified solar radiation, and used the present state to determined the appropriate bulk coefficients appearing in the model.

In spite of the model limitations, the qualitative nature of the Younger Dryas climate event has been reproduced. Our results strongly support the idea that this event reflects reduced overturning in the Atlantic as a result of meltwater input as suggested by Broecker et al. (1988). The change made in the present study compared to past studies that results in a much better simulation is a relatively minor, temporally invariant, modification of the atmospheric branch of the hydrological cycle. The modification corresponds to a 35% reduction in the model estimate of runoff into the North Atlantic, but this difference may be due to model and data inaccuracies rather than a real reduction in runoff. The important point is that the qualitative nature of the Younger Dryas event is as one would expect due to meltwater input for conditions which are not far removed from the present state. Improved representations could almost certainly be achieved by addressing some of the questions raised in the previous paragraphs, but a detailed simulation is not the purpose of the present investigation.

It is interesting that the modification of the hydrological cycle which gives a realistic duration of the Younger Dryas event also results in a minimal response to the second meltwater pulse, consistent with observations. This large difference in response to the first and second meltwater pulses is a consequence of the first pulse having sufficient strength and duration to reduce the North Atlantic surface salinity beyond the critical point where convection is terminated, whereas the second pulse did not exceed this critical point.

The model simulation shows a collapse of the Atlantic overturning circulation very near the first meltwater peak, somewhat earlier than recent observations suggest (Lehman and Keigwin, 1992). This may be due in part to our idealization of adding all of the meltwater to the Atlantic between 20 and 32.5°N. More realistic geographic and temporal variations should be considered. Other effects that might have delayed the collapse include zonal variations in water mass formation, a more localized atmospheric response around the North Atlantic to reduced oceanic heat transport, the influence of brine rejection associated with seasonal cycles in sea ice extent, and albedo feedbacks that are neither accounted for in our initial state nor in our transient simulation.

In our most realistic simulation, the Younger Dryas event lasted for roughly 1000y and then spontaneously and abruptly terminated. It should be emphasized that the model estimate of the length of this event is a tunable characteristic. This time is determined by the rate at which the fresh water cap over the North Atlantic is removed after meltwater input is terminated, and this depends principally on the atmospheric branch of the hydrological cycle and the north-south exchange of water. A relatively small modification of the present-day hydrological cycle results in reasonable agreement between the model simulation and observations: the change is certainly within the model uncertainty.

An even smaller change in the hydrological cycle would be required if horizontal exchange of near surface waters were enhanced during the period of collapsed circulation. In our model, horizontal diffusion is the primary mechanism by which the fresh water lens is eroded away after meltwater input is reduced and hence increasing this quantity, particularly the near-surface values, will reduce the length of the model's Younger Dryas event. In this regard, it should be noted that horizontal diffusion in the present model accounts for both mesoscale eddies and the basin scale gyre circulations due to wind forcing. Winton and Sarachik (1992) note that the Sverdrup transport will be concentrated more in the surface layer if the thermohaline circulation collapses, resulting in a stronger near-surface gyre circulation. In our model this should be represented by an increase in $K_H$ in the near surface region. Test runs in which $K_H$ was simply increased by $500\text{-}1000 m^2 s^{-1}$ during the period of collapsed circulation confirm that this results in more rapid removal of the fresh water lens and a smaller reduction of $R$ to fit the model to the observed length of the Younger Dryas event. Some decrease in $R$ was still required for the overturning circulation to re-initiate, but values as large as 0.8 gave reasonable results when $K_H$ was increased by $1000 m^2 s^{-1}$ during the collapsed period. This corresponds to a 20% decrease in the model estimate of 'runoff' which is negligible in comparison with expected errors in the model predictions and the data.

The very abrupt recovery of the overturning circulation is also consistent with observations (Dansgaard et al., 1989). This is a consequence of positive feedbacks which operate during the period of increasing overturning. Both reduced residence time of the high latitude surface waters and, more importantly, the upward flux of saline water due to convection contribute to the rapid rejuvenation of the overturning circulation and consequently the rapid termination of the Younger Dryas event.

## References

Baumgartner A, Reichel E (1975) The World Water Balance, Elsevier, New York, 179p.

Birchfield GE (1990) A salt oscillator in the glacial Atlantic? 2. A "scale analysis" model. Paleoceanography 5: 835-843.

Boyle EA, Keigwin LD (1982) Deep circulation of the North Atlantic over the last 200,000 years: geochemical evidence. Science 218: 784-787.

Boyle EA, Keigwin LD (1987) North Atlantic thermohaline circulation during the past 20,000 years linked to high-latitude surface temperature. Nature 330: 35-40.

Broecker WS, Peteet DM, Rind D (1985) Does the ocean-atmosphere system have more than on stable mode of operation? Nature 315: 21-26.

Broecker WS, Andree M, Wolfli W, Oeschger H, Bonani G, Kennett J, Peteet D (1988) The Chronology of the last deglaciation: Implications to the cause of the Younger Dryas event. Paleoceanogr. 3: 1-19.

Bryan F (1986) High-latitude salinity effects and interhemispheric thermohaline circulations. Nature 323: 301-304.

Budyko MI (1969) The effect of solar radiation variations on the climate of the earth. Tellus 21: 611-619.

CLIMAP Project Members (1981) Seasonal reconstruction of the Earth's surface at the last glacial maximum. Geol. Soc. Amer.; Map and Chart Series 36.

Dansgaard W, White JWC, Johnsen SJ (1989) The abrupt termination of the Younger Dryas climate event. Nature 339: 532-534.

Duplessey JC, Labeyrie L, Arnold M, Paterne M, Duprat J, van Weering TCE (1992) Changes in surface salinity of the North Atlantic Ocean during the last deglaciation. Nature 358: 485-488.

Fairbanks RG (1989) A 17,000-year glacio-eustatic sea level record: Influence of glacial melting rates on the Younger Dryas event and deep-ocean circulation. Nature 342: 637-642.

Fairbanks RG (1990) The age and origin of the "Younger Dryas Climate Event" in Greenland ice cores. Paleoceanogr. 5: 937-948.

Gill AE (1982) Atmosphere-Ocean Dynamics. Academic Press, 662pp.

Gordon AL (1986) Interocean exchange of thermocline water. J. Geophys. Res. 91: 5037-5046.

Han YJ, Lee SW (1983) An analysis of monthly mean wind stress over the global ocean. Mon. Weather Rev. 111: 1554-1566.

Haney RL (1971) Surface thermal boundary condition for ocean circulation models. J. Phys. Oceanogr. 1: 241-248.

Hastenrath S (1982) On the meridional heat transport in the world ocean. J. Phys. Oceanogr. 12: 922-927.

Hsiung J (1985) Estimates of global oceanic meridional heat transport. J. Phys. Oceanogr. 15: 1405-1413.

Jansen E, Veum T (1990) Evidence for two-step deglaciation and its impact on North Atlantic deep-water circulation. Nature 343: 612-616.

Kallel N, Labeyrie LD, Arnold M, Okada H, Dudley WC, Duplessey J-C (1988) Evidence of cooling during the Younger Dryas in the western North Pacific. Oceanol. Acta 11: 369-375.

Kundrass HR, Erlenkeuser H, Vollbrecht R, Weiss W (1991) Global nature of the Younger Dryas cooling event inferred from oxygen isotope data from Sulu Sea cores. Nature 349: 406-409.

Kutzbach JE, Guetter PJ (1986) The influence of changing orbital parameters and surface boundary conditions on climate simulations for the past 18000 years. J. Atmos. Sci. 43: 1726-1759.

Lehman SJ, Keigwin LD (1992a) Sudden changes in the North Atlantic circulation during the last deglaciation. Nature 356: 757-762.

Levitus S (1982) Climatological atlas of the world ocean. NOAA Prof. Paper, 13, 173pp.

Maier-Reimer E, Mikolajewicz U (1989) Experiments with an OGCM on the cause of the Younger Dryas. In Oceanography, A. Ayala-Castanares, W. Wooster and A. Yanez-Arancibia (eds.), UNAM Press, 87-100.

Manabe S, Stouffer RJ (1988) Two stable equilibria of a coupled ocean-atmosphere model. J. Climate 1: 841-866.

Marotzke J, Willebrand J (1991) Multiple equilibria of the global thermohaline circulation. J. Phys. Ocenaogr. 21: 1372-1385.

Miller JR, Russell GL (1990) Oceanic freshwater transport during the last glacial maximum. Paleoceanography 5:397-407.

North GR, Mengel JG, Short DA (1983) Simple energy balance model resolving seasons and the continents: applications to the astronomical theory of the ice ages. J. Geophys. Res. 88: 6576-6586.

Oort AH (1983) Global atmospheric circulation statistics, 1958-1973. NOAA Prof. Paper No. 14: 180pp.

Rind D, Peteet D, Broecker W, McIntyre A, Ruddiman W (1986) The impact of cold North Atlantic sea surface temperatures on climate: Implications for the Younger Dryas cooling (11-10K). Clim. Dyn. 1: 3-33.

Ruddiman WF, McIntyre A (1981) The North Atlantic Ocean during the last deglaciation. Paleogeogr. Paleoclimatol. Paleoecol. 35: 145-214.

Ruddiman WF, Duplessey JC (1985) Conference on the last deglaciation: Timing and mechanism, Quat. Res. 23: 1-17.

Sellers WD (1969) A global climatic model based on the energy balance of the earth-atmosphere system. J. Appl. Meteor. 8: 392-400.

Semtner AJ (1976) A model for the thermodynamic growth of sea ice in numerical investigations of climate. J. phys. Oceanogr. 6: 379- 389.

Stephens GL, Campbell GG, Vonder Haar TH (1981) Earth radiation budgets. J. Geophys. Res. 86: 9739-9760.

Stocker TF, Wright DG (1991a) A zonally averaged ocean model for the thermohaline circulation. Part II: Interocean circulation in the Pacific-Atlantic basin system. J. Phys. Oceanogr. 21: 1725-1739.

Stocker TF, Wright DG (1991b) Rapid transitions of the ocean's deep circulation induced by changes in surface water fluxes. Nature 351: 729-732.

Stocker TF, Wright DG, Mysak LA (1992) A zonally averaged, coupled ocean-atmosphere model for paleoclimate studies. J. Clim. 5: 773-797.

Talley LD (1984) Meridional heat transport in the Pacific Ocean. J. Phys. Oceanogr. 14: 231-241.

Veum T, Jansen E, Arnold M, Beyer I, Duplessey J-C (1992) Water mass exchange between the North Atlantic and the Norwegian Sea during the past 28,000 years. Nature 356: 783-785.

Winton M, Sarachik ES (1993) Thermohaline oscillations induced by strong steady salinity forcing of ocean general circulation models. J. Phys. Oceanogr. (in press)

Wright DG, Stocker TF (1991) A zonally averaged ocean model for the thermohaline circulation. Part I: Model development and flow dynamics. J. Phys. Oceanogr., 21: 1713-1724.

Wright DG, Stocker TF (1992) Sensitivities of a zonally averaged global ocean circulation model. J. Geophys. Res. 97: 12707-12730.

Zaucker F (1992) Observed versus modelled freshwater fluxes and their impact on the global thermohaline circulation. PhD Thesis, Ruprecht-Karls-Universitat, Heidelberg.

Zahn R (1992) Deep ocean circulation puzzle. Nature 356: 744-746.

Zhang S, Greatbatch RJ, Lin CA (1993) A re-examination of the polar halocline catastrophe and implications for coupled ocean-atmosphere modelling. J. Phys. Oceanogr. (in press)